# ACM/Hindered Phenol Hybrids: A High Damping Material with Constrained-Layer Structure for Dynamic Mechanical Analysis and Simulation

Cong Li*, Xiaoxia Cai, Chifei Wu and Guozhang Wu

*Polymer Alloy Laboratory, School of Materials Science and Engineering, East China University of Science and Technology, 130 Meilong Rd., Shanghai 200237, P.R. China*

**Abstract:** Due to the strong hydrogen bonding interactions, hindered phenol 3,9-bis[1,1-dimethyl-2{*β*-(3-tert-butyl-4-hydroxy-5- methylphenyl)propionyloxy}ethyl]- 2,4,8,10-tetraoxaspiro[5,5]-undecane (AO-80) demonstrated a remarkable damping effect when it was hybridized with acrylic rubber (ACM). The loss factor of ACM could be largely increased and the position of loss peak could be regulated by controlling the content of the hindered phenol. This kind of high damping hybrids can be used as the laminated layer of sandwich beam for vibration control. Instead of the traditional method ASTM E756-98, a new method based on dynamic mechanical analyzer (DMA) was developed to characterize the damping behaviors of ACM/AO-80 laminated beam. Testing results demonstrated that DMA can reflect the variation of damping behaviors of sandwich beams with various factors effectively, and a theoretical model established here was used to explain the damping behaviors. Based on this model, by means of adjusting the content of AO-80, a high damping ability for the sandwich beam could be obtained at appointed temperature during a wide frequency range.

**Keywords:** Damping behavior, Hindered phenol, Loss peak, Simulation.

## 1. INTRODUCTION

In the last decades, polymer is widely used in the field of low-frequency vibration and noise control, due to its high damping potential at the glass transition. Many approaches have been reported to broaden the glass-transition temperature (*Tg*), which can further improve the effective damping range. One of the most conventional ways is to mix several kinds of polymers with different *Tg* [1-3]; Interpenetrating polymer network (IPN) in which the phase-separated domain is limited to a very small size has been conformed to be a very effective structure as high-performance damping materials [4-6]; Addition of inorganic filler in polymer matrix is also a quite useful method to improve the damping behavior due to the friction between the filler and the chains of polymer [7-8]. Another concept is based on hybrid of a bifunctional small molecule with a polar polymer to control the microphase separation and crystallization of the added small molecules in the polymer matrix [9-12]. Not only the loss peak is improved, but also the effective damping range is broadened.

In practical application, the polymeric damping materials are always laminated with other stiff sheets such as steel and aluminum. There are two main forms of damping treatments. One is extensional damping referred to as the free-layer damping treatment. The other is shear damping referred to as the constrained-layer damping treatment. Generally, the vibration damping properties of laminated beams can not be measured directly but instead are deduced from the response characteristics of them [13]. One measure of damping, known as the logarithmic decrement, is related to the ratio of the nth to the n+Nth cycle amplitudes of a cantilever beam which is deformed and then released from rest. The other method is the standard ASTM E 756-98, which is the common method of measuring the vibration damping property of a beam. The loss factor can be calculated around each resonance peak using the half-power bandwidth method [14, 15]. It should be pointed out that determination of the vibration damping behavior by these methods requires specialized and complicated measuring system, and the measurement is very expensive.

The objective of this paper is to provide a simpler and cheaper method for investigating the damping behaviors of sandwich beams and to develop optimized sandwich beam structure having high damping property at appointed temperature during a frequency range (1 Hz ~ 600 Hz). This work consists of three parts. Firstly, we developed a new kind of organic hybrid with high-damping performance and self-adhesive characteristic suitable as the damping layer of a sandwich beam; secondly, dynamic mechanical analyzer (DMA) was used to measure the vibration damping behaviors of sandwich beams. Finally, a theoretical model was established to characterize the vibration damping behaviors of sandwich beams.

*Address correspondence to this author at the Polymer Alloy Laboratory, School of Materials Science and Engineering, East China University of Science and Technology, 130 Meilong Rd., Shanghai 200237, P.R. China; Tel: +86 531 8963 1227; E-mail: li.cong80@yahoo.com

**E-ISSN: 1929-5995/16** 

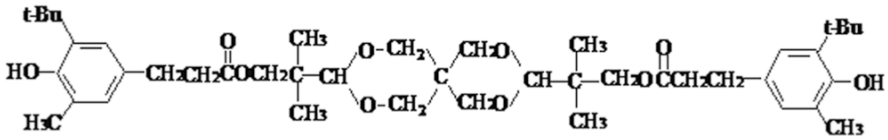

**Figure 1:** Chemical structure of AO-80.

## 2. EXPERIMENTAL

### 2.1. Raw Materials

Acrylic rubber (ACM) used in this study is a commercial grade (Nippl AR54, Nippon Zeon Co.). Hindered phenol 9-bis[1,1-dimethyl-2{*β*-(3-tert-butyl-4-hydroxy-5-methylphenyl) propionyloxy}ethyl]-2,4,8,10-tetraoxaspiro[5,5]-undecane (AO-80, as shown in Figure **1**) used as functional additive is a kind of commercial antioxidant (ADK STAB AO-80; Asahi Denka Industries Co.).

### 2.2. Sample Preparation

The ACM were kneaded by mixing rollers for 5 minutes, and then, the AO-80 was added. The kneaded mixtures were compression moulded into sheets under a pressure of 10 MPa for 10 minutes at 150°C. The thickness of the prepared sheet was about 2 mm, and was used as the damping layer material. Here, aluminum sheet was chosen as the constraining layer. Because of the self-adhesive property for the ACM/AO-80 hybrid, the constraining layer can be bonded with the ACM/ AO-80 hybrid directly. The sandwich was achieved by pressing the constraining layer laminated with a damping layer under 0.2 MPa pressure at room temperature. The thickness of the damping layer was controlled by the pressing time, and 4 samples with different damping layer components were prepared as listed in Table **1**.

### 2.3. Dynamic Mechanical Analysis (DMA)

Because the damping layer undergoes pure shear in the sandwich structure, solid shear mode was selected to measure the dynamic mechanical properties of ACM/ AO-80 hybrids with a strain set at 0.07% [14] by the dynamic mechanical analyzer (Rheogel-E4000; UBM Co.). Specimens for the measurements were prepared as 6 mm in length, 6mm in width, and 2 mm in thickness. The temperature dependence of tan *δ* was measured at a constant frequency of 11 Hz with a heating rate of 3°C/min, and the frequency dependence of dynamic shear modulus and tan *δ* was measured during a frequency range from 1 Hz to 600 Hz at a series of temperatures.

DMA is a powerful tool for measuring the variation of loss factor of a material with many factors and has been widely used by researchers. Therefore, an attempt was made here to measure the vibration damping behaviors of sandwich beams by DMA. In practice, the ends of many apparatuses are fixed and there is a vibration in the middle of the body. So, the sandwich beam tested here has a boundary condition that both ends of the beam are clamped with a concentrated sinusoidal load $P_0e^{i\omega t}$ applied at the midpoint of the constraining layer as depicted in Figures **2** and **3** shows the dynamic mechanical analyzer (Rheogel-E4000; UBM Co.) installed with the sandwich beam, and the testing conditions are listed in Table **1**.

**Table 1: Dimensions and Testing Conditions of the Tested Samples**

| Sample Code | Length (mm) | Width (mm) | Thickness (mm) | | Composition of the Damping Layer | Composition of the Constraining Layer | Measuring Temperature (°C) | Measuring Frequency (Hz) |
|---|---|---|---|---|---|---|---|---|
| | | | Damping Layer | Constraining Layer | | | | |
| 1 | 30 | 4 | 0.10 | 0.78 | ACM/AO-80 (100:40) | Al | 0°C~50°C | 1Hz~600Hz |
| 2 | 30 | 4 | 0.10 | 0.78 | ACM/AO-80 (100:80) | Al | 0°C~50°C | 1Hz~600Hz |
| 3 | 30 | 4 | 0.10 | 0.78 | ACM/AO-80 (100:120) | Al | 0°C~50°C | 1Hz~600Hz |
| 4 | 30 | 4 | 0.10 | 0.78 | ACM/AO-80 (100:160) | Al | 0°C~50°C | 1Hz~600Hz |

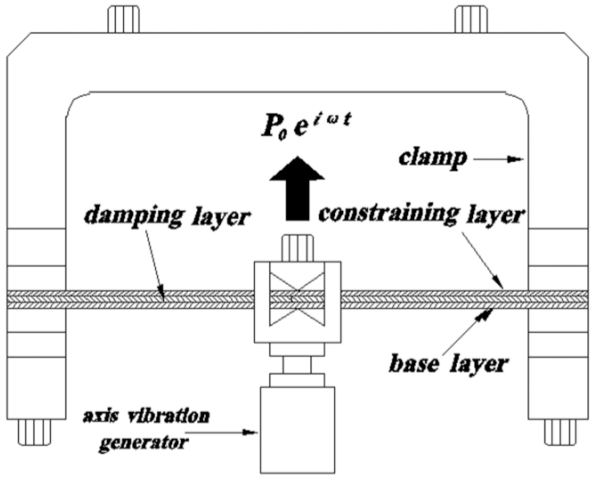


**Figure 2:** Sketch of the sandwich beam under a clamped-clamped boundary condition.

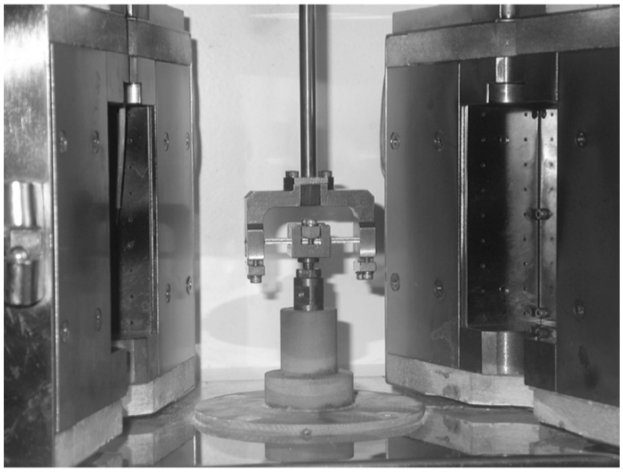

**Figure 3:** Dynamic mechanical analyzer (Rheogel-E4000; UBM Co.) used in the investigation.

## 3. RESULTS AND DISCUSSION

### 3.1. Viscoelastic Properties of ACM/AO-80 Hybrids

Figure **4** shows the temperature dependence of the loss factor (tan *δ*) at11 Hz for ACM hybrids added with different content of AO-80. As shown in the figure, a high single tan *δ* peak appears after the addition of AO-80, demonstrating that AO-80 is compatible with ACM. Moreover, the maximum value of the tan *δ* peak increases and the peak location shifts to higher temperature with increasing the content of AO-80. These phenomena can be attributed to the dissociation of the hydrogen bonds of AO-80 [10, 16] and the existence of intermolecular hydrogen bonds between ACM and AO-80 [17]. Kerwin indicated that a higher loss factor of viscoelastic materials will conduce to the damping capacity of sandwich [18]. Therefore ACM/AO-80 hybrids are used as the damping layer in this investigation.

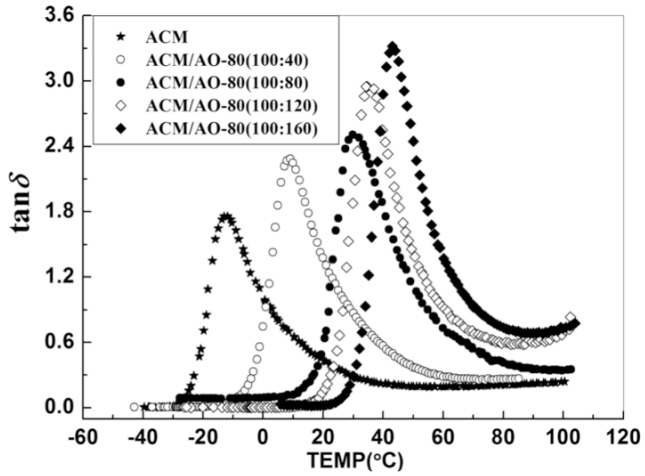


**Figure 4:** The temperature dependence of loss factor (tan *δ*) at 11Hz for ACM and ACM/AO-80 hybrids.

It is well known that the damping property of a polymer is determined by the cooperation of temperature and frequency. The temperature dependence of tan *δ* at 11Hz for ACM/AO-80 hybrids is shown in Figure **4**. In order to reveal the influence of frequency on the damping peaks, the time-temperature superposition principle was used and the William–Landel–Ferry (WLF) equation was applied to obtain the master curves for the shear loss tangent over a wide frequency range. A series of measurements on frequency dependence of dynamic mechanical properties were performed at various temperatures near the corresponding glass transition temperature for ACM/AO-80 hybrids. The testing frequencies for these measurements were in the range from 1 Hz to 600 Hz. In accordance with these results, the constants in the WLF equation were obtained as C1≈101 and C2≈17.

Figure **5** exhibits master curves of the shear loss tangent vs frequency for various ACM/AO-80 hybrids with respect to reference temperatures near the corresponding glass transitions. If tan *δ* ≥1 is taken as the criterion for a high damping property, it can be found from this figure that the high damping demand can be satisfied during a frequency range from 1 Hz to 800 Hz. Therefore, the following measurement for the sandwich beam is carried out from 1Hz to 600Hz (considering the DMA security, the frequency value should not be set too high).

### 3.2. Vibration Damping Behaviors of Sandwich Beams

Figure **6** shows the variation of structural loss factor $\eta_s$ with frequency for sandwich beam laminated with ACM/AO-80 (100:40) at different temperatures. It can

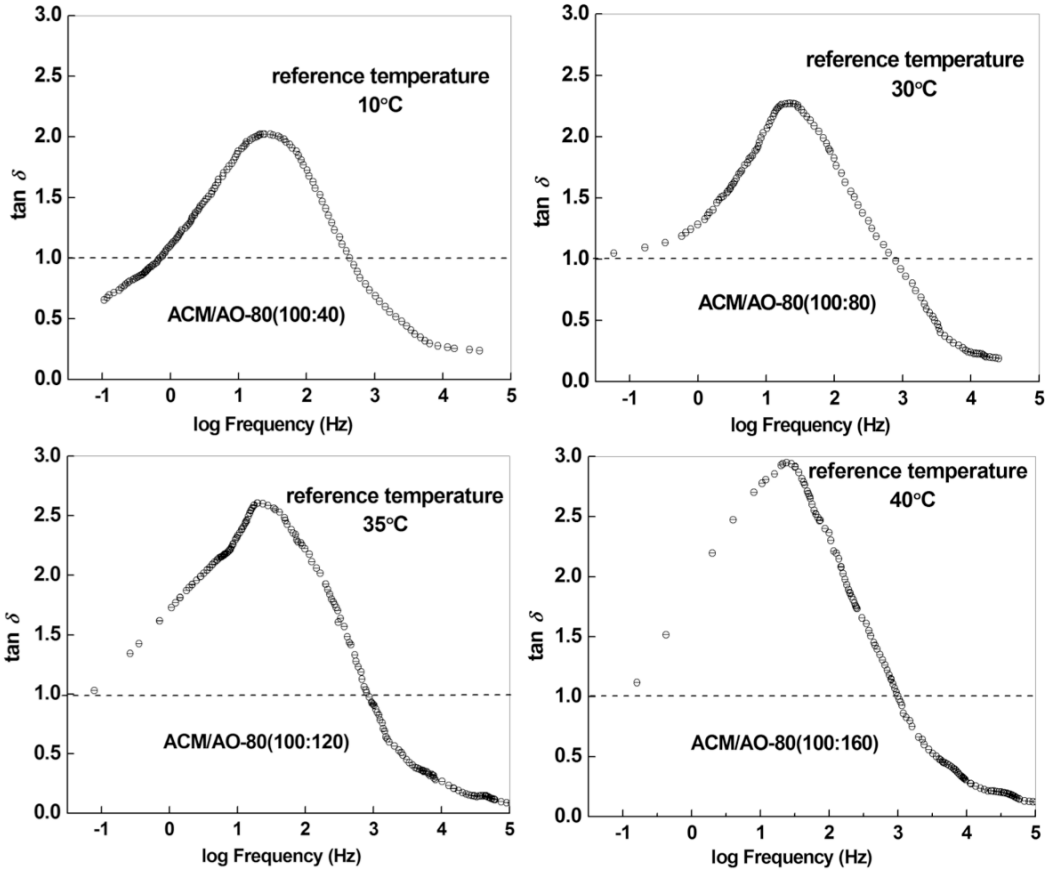


**Figure 5:** Frequency dependence of loss tangent for ACM/AO-80 hybrids with respect to reference temperatures near the corresponding glass transitions.

be seen from this figure that the tendency of $\eta_s$ with frequency varies considerably at different temperatures. At 0°C, the $\eta_s$ decreases with frequency, whereas the $\eta_s$ keeps increasing with frequency at 10°C, and it increases at first then decreases with frequency at 5°C. This phenomenon indicates that the $\eta_s$ of the sandwich beam is affected by temperatures and frequencies significantly. If a frequency range from 1 Hz to 600 Hz is selected for damping application, 5°C is preferable than other two temperatures.

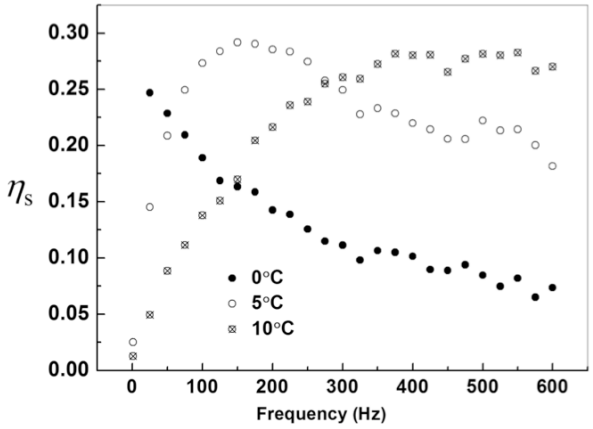


**Figure 6:** Variation of structural loss factor $\eta_s$ with frequency for sandwich beam laminated with ACM/AO-80 (100:40) at different temperatures.

Figure **7** shows the variation of structural loss factor $\eta_s$ with frequency for sandwich beams having different damping layer components at 20°C. It can be seen from this figure that different content of AO-80 in organic hybrids lead to distinct vibration damping behaviors. When the content of AO-80 is increased from 40 phr to 80 phr, a $\eta_s$ peak appears and the $\eta_s$ of it is much higher than that of the sandwich beam laminated with ACM/AO-80 (100:40). This means the ACM/AO-80 (100:80) laminated beam has better damping ability at 20°C during a frequency range from 1Hz to 600Hz.

DMA test results show that sandwich beams exhibit different vibration damping behaviors with the variation of temperature, frequency, and composition of the damping layer. Though the method proposed here is different from the standard ASTM E 756-98, it can reflect the variation of structural loss factor with various

factors. The correlation between the two methods will be investigated in the next work.

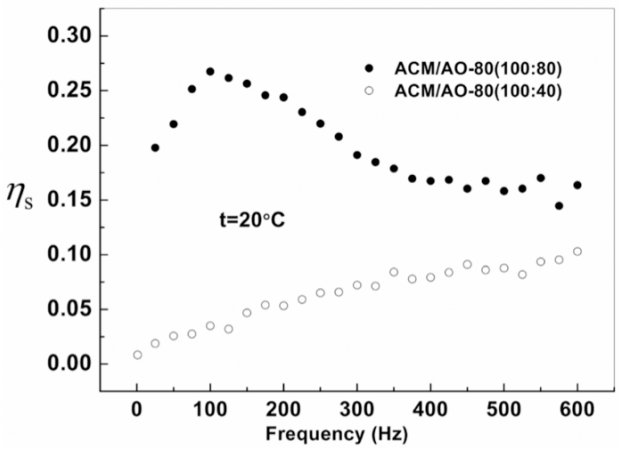


**Figure 7:** Variation of structural loss factor $\eta_s$ with frequency for sandwich beams laminated with different composition at 20°C.

## 4. THEORETICAL ANALYSIS

In order to illustrate the phenomena mentioned above and characterize the damping behavior of the sandwich beam, a theoretical model was established. The damping of a system under steady state vibration can be expressed by the structural loss factor, which is the ratio of the energy dissipated per cycle to the maximum strain energy in the system [13]. That is,

$$\eta_S = \Delta W/2\pi W_S \tag{1}$$

The calculation of $\Delta W$ could be conducted using an energy consuming model proposed by Plunkett [19].

$$\Delta W = 2\pi h_2 E_2 L \varepsilon_0^{\,2} \frac{1}{\omega} \left\{ \frac{sinh\left[\omega cos\left(\theta/2\right)\right] sin\left(\theta/2\right) - sin\left[\omega sin\left(\theta/2\right)\right] cos\left(\theta/2\right)}{cosh[\omega cos\left(\theta/2\right)] + cos[\omega sin\left(\theta/2\right)]} \right\} \tag{2}$$

Where $\omega = \frac{L}{\sqrt{h_1 h_2 E_2 / G^*}}$, $h_1$ and $h_2$ are the thickness of the damping layer and the constraining layer separately; $E_2$ is the modulus of elasticity of the constraining material; $L$ is the length of the sandwich beam; $G^*$ ($G^* = \sqrt{\left(G'\right)^2 + \left(G''\right)^2}$) is the effective shear modulus of the viscoelastic material; $\varepsilon_0$ is the uniform strain at the interface of the base layer, and $\theta$ is the loss angle of the viscoelastic material ($\tan\theta = \tan\delta$).

The maximum strain energy in a constraining layer can be expressed [20].

$$w_2 = \frac{E_2 I_2}{2} \int_0^L \left( \frac{d^2 y}{dx^2} \right)^2 dx = \frac{E_2 h_2^{\,3}}{24} \int_0^L \left( \frac{d^2 y}{dx^2} \right)^2 dx = \frac{E_2 h_2^{\,3} L}{24} \frac{1}{\rho_2^{\,2}} \tag{3}$$

The maximum strain energy in a base layer has the similar formation

$$w_3 = \frac{E_3 I_3}{2} \int_0^L \left( \frac{d^2 y}{dx^2} \right)^2 dx = \frac{E_3 h_3^{\,3}}{24} \int_0^L \left( \frac{d^2 y}{dx^2} \right)^2 dx = \frac{E_3 h_3^{\,3} L}{24} \frac{1}{\rho_3^{\,2}} \tag{4}$$

Where $I_2$ and $I_3$ are moments of inertia of the constraining and base layer, separately; $\rho_2$ and $\rho_3$ are curvature radii of the constraining and base layer, separately. Due to the much lower modulus of the damping layer compared with that of the constraining layer, the maximum strain energy in the damping layer is negligible. Thus, the maximum strain energy of the system can be represented as:

$$W_S = w_2 + w_3 = \frac{E_2 h_2^{\,3} L}{24} \frac{1}{\rho_2^{\,2}} + \frac{E_3 h_3^{\,3} L}{24} \frac{1}{\rho_3^{\,2}} \tag{5}$$

Because the laminate is symmetric, the base layer is equal to the constraining layer, and $E_2 = E_3$, $h_2 = h_3$. Therefore,

$$W_S = w_2 + w_3 = \frac{E_2 h_2^{\,3} L}{24} \left( \frac{1}{\rho_2^{\,2}} + \frac{1}{\rho_3^{\,2}} \right) \tag{6}$$

The strain at the interface of the base layer and the damping layer is

$$\varepsilon_0 = -\left(h_3/2\right)\left(d^2 y/dx^2\right) = -\left(h_3/2\right)\left(1/\rho_3\right) \tag{7}$$

So eq. (2) can be written as:

$$\Delta W = 2\pi h_2 E_2 L \left( h_3^{\,2} / 4\rho_3^{\,2} \right) \frac{1}{\omega} \left\{ \frac{sinh\left[\omega cos\left(\theta/2\right)\right] sin\left(\theta/2\right) - sin\left[\omega sin\left(\theta/2\right)\right] cos\left(\theta/2\right)}{cosh[\omega cos\left(\theta/2\right)] + cos[\omega sin\left(\theta/2\right)]} \right\} \tag{8}$$

Substituting eqs. (8) and (6) into eq. (1), finally, the expression of the structural loss factor is obtained:

$$\eta_s = \Delta W/2\pi W_s = m \frac{1}{\omega} \left\{ \frac{sinh\left[\omega cos\left(\theta/2\right)\right] sin\left(\theta/2\right) - sin\left[\omega sin\left(\theta/2\right)\right] cos\left(\theta/2\right)}{cosh[\omega cos\left(\theta/2\right)] + cos[\omega sin\left(\theta/2\right)]} \right\} \tag{9}$$

Where, $m = \frac{6\left(1/\rho_3^2\right)}{\left(1/\rho_3^2 + 1/\rho_2^2\right)}$.

Figure **8a** and **8b** separately show the comparison between the measured values and calculated values based on eq.(9) for sandwich beams laminated with ACM/AO-80(100:40) and ACM/AO-80(100:80). The *G** and tan$\theta$ of the damping layer materials used in eq.(9) are shown in Figures **9** and **10**, separately. Because the storage modulus of the constraining layer is insensitive to the testing frequency, according to DMA test data, the value is set to 5.3×10$^{10}$ Pa. An agreement between the measured values and the calculated values derived from eq. (9) can be found in Figure **8**.

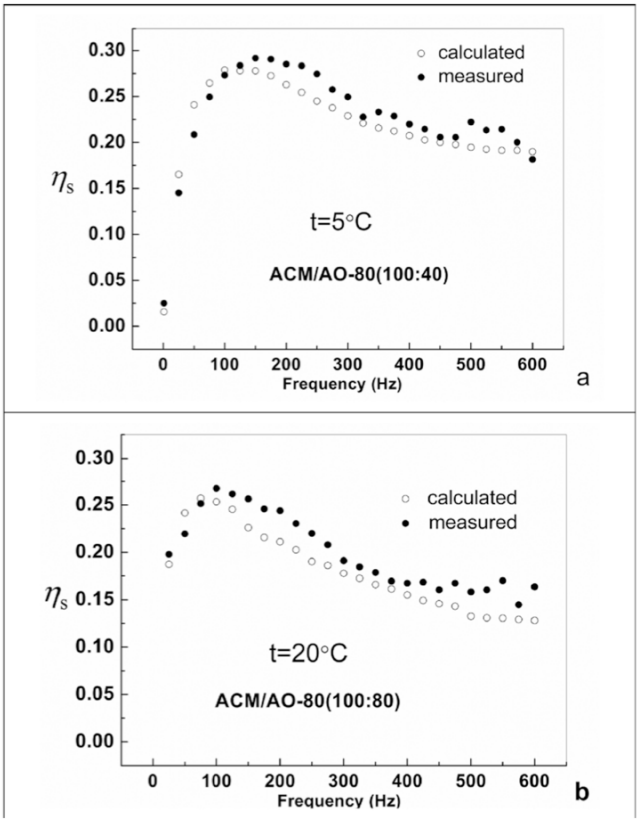


**Figure 8:** Comparison between the measured values and calculated values for sandwich beams laminated with ACM/AO-80(100:40) or ACM/AO-80(100:80).

Figure **11** describes the variation of $\eta_s$ with the shear modulus and loss angle of the damping layer materials based on eq.(9) for sandwich beam laminated with ACM/AO-80 (100:40). It can be found the *G** corresponding to the maximum $\eta_s$ in Figure **11** is 2.2×10$^7$ Pa. This implies that in order to obtain a high damping property for the sandwich beam, a shear modulus *G** near 2.2×10$^7$ Pa is needed. Figure **12** shows the variation of *G** with frequency at different temperatures for ACM/AO-80(100:40). It can be found

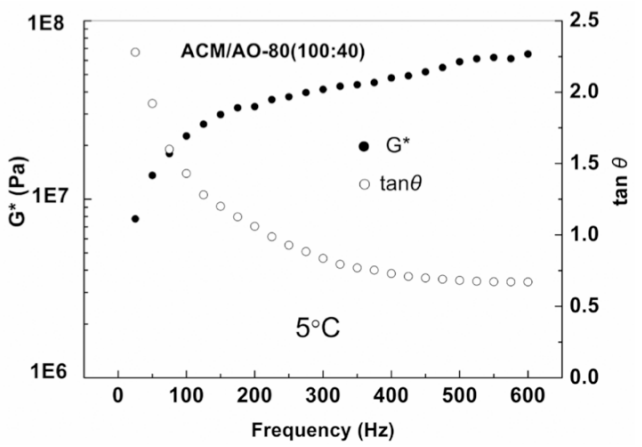


**Figure 9:** Frequency dependence of G* and tan$\theta$ at 5°C for ACM/AO-80 (100:40).

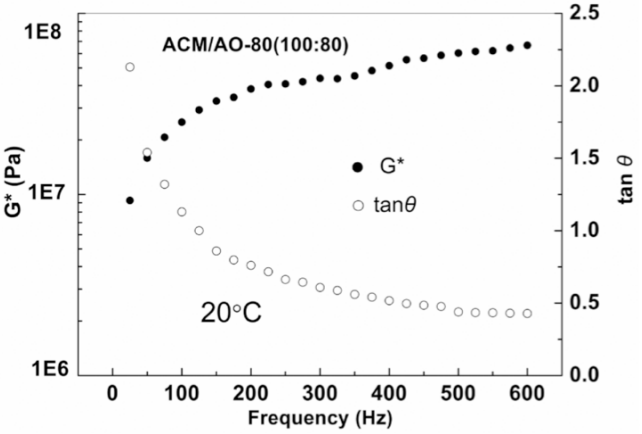


**Figure 10:** Frequency dependence of G* and tan$\theta$ at 20°C for ACM/AO-80 (100:80).

from this figure that the frequencies corresponding to the modulus (2.2×10$^7$ Pa) are quite distinct at different temperatures. When the temperature is 5°C, the frequency with a corresponding modulus 2.2×10$^7$ Pa is located near 120Hz, whereas a higher frequency is needed at 10°C and a lower frequency is necessary at 0°C. Thus, a $\eta_s$ peak will appears near 120Hz when the temperature is 5°C, and the measured result shown in Figure **6** testifies the prediction. Because when the temperature is 10°C, a higher frequency is needed for ACM/AO-80 with a shear modulus *G** 2.2×10$^7$ Pa, the $\eta_s$ increases with the frequency increases (shown in Figure **6**) is easy to understand. Analogously, the $\eta_s$ will decrease with the increase of frequency when the temperature is 0°C. A similar tendency based on eq.(9) can be deduced for sandwich beam laminated with ACM/AO-80 (100:80).

The discussion above proves that the vibration damping behaviors of sandwich beams can be characterized according to the model established here,

and the phenomena measured by DMA were illustrated by this model.

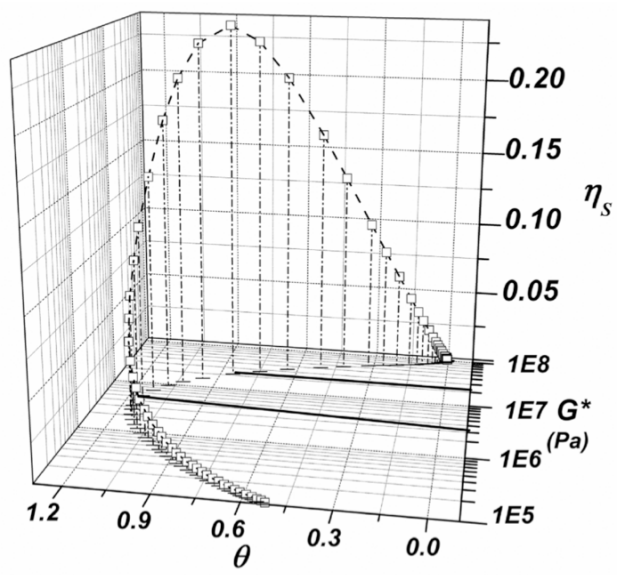


**Figure 11:** Variation of $\eta_s$ with the shear modulus and the loss angle of the damping layer material based on eq. (9) for sandwich beam laminated with ACM/AO-80 (100:40).

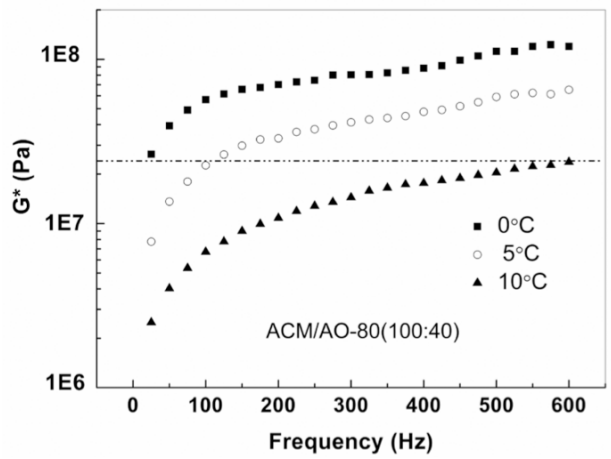


**Figure 12:** Frequency dependence of G* for ACM/AO-80 (100:40) at different temperatures.

## 5. DESIGNING SANDWICH BEAMS

Generally speaking, the higher the loss factor of the damping layer material, the more favorable for the enhancement of the structural loss factor of a sandwich beam. Figure **4** shows a tan *δ* peak exists for ACM/AO-80 (100:40) at 11Hz when the temperature is 10°C. However, we can find from Figure **6** that when the temperature is set as 10°C, there is no $\eta_s$ peak appearing for ACM/AO-80 (100:40) laminated sandwich beam during a frequency range from 1Hz to 600Hz. This means there is not the necessity that the maximum loss factor of a damping layer material leads to the maximum structural loss factor of the corresponding sandwich beam. As it is shown in Figure **11**, there is a discrepancy between the loss angle peak and the structural loss factor peak. When the loss angle of the damping layer reaches the maximum value 1.159, the corresponding modulus is $3.2\times10^6$ Pa, whereas the maximum structural loss factor needs a higher corresponding modulus ($2.2\times10^7$ Pa) and the corresponding loss angle is 0.85. Therefore, in addition to the loss factor of the damping layer material, shear modulus *G** is another important element affecting the structural loss factor. Compared with the corresponding modulus of the maximum loss angle of the damping layer material, a higher modulus of the maximum structural loss factor implies that the $\eta_s$ peak will appear at a lower temperature, provided that the frequency is the same.

We can find from Figure **6** that a relatively high $\eta_s$ ($\eta_s$ > 0.2) can be maintained during a frequency range from 50 Hz to 550 Hz at 5°C. This damping property can not be obtained at other temperatures when the frequency is confined in a range from 1 Hz to 600 Hz. If ACM/AO-80 (100:40) is selected as the damping layer material, and the frequency is limited in a range no higher than 600Hz, 5°C is preferential than other temperatures. As mentioned above, temperature appearing the $\eta_s$ peak is always lower than the temperature appearing the tan *δ* peak of the corresponding damping layer material, in order to obtain a high damping property for the sandwich beam over a wide frequency range near room temperature, the loss factor peak of the ACM/AO-80 need shift to a temperature higher than room temperature. Because the compatibility between the AO-80 and ACM, and the inherent high damping property of AO-80 [16] at a relatively high temperature, the addition of AO-80 in the ACM matrix can make damping peak shifts to a higher temperature and high damping peaks can be obtained as shown in Figure **4**. Thus ACM/AO-80 hybrids mixed with different content of AO-80 are selected as the damping layer materials for sandwich beam. Figure **13** shows the damping behaviors of sandwich beams laminated with different ACM/AO-80 hybrids at a series of pointed temperatures during a frequency range from 1Hz to 600Hz. For the comparison convenience, the calculated values derived from eq.(9) are also listed in Figure **13**. It can be found from this figure that a relatively higher structural loss factor appears within a certain temperature range, beyond this temperature range, the structural loss factors drop rapidly. With the increase of the AO-80 content, the structural loss factor peak shifts to a higher temperature, especially ACM/AO-80 (100:80) laminated sandwich beam has a high damping property near room temperature. It can be also found from Figure **13** that the variation tendency of the $\eta_s$ peak temperature with the increase

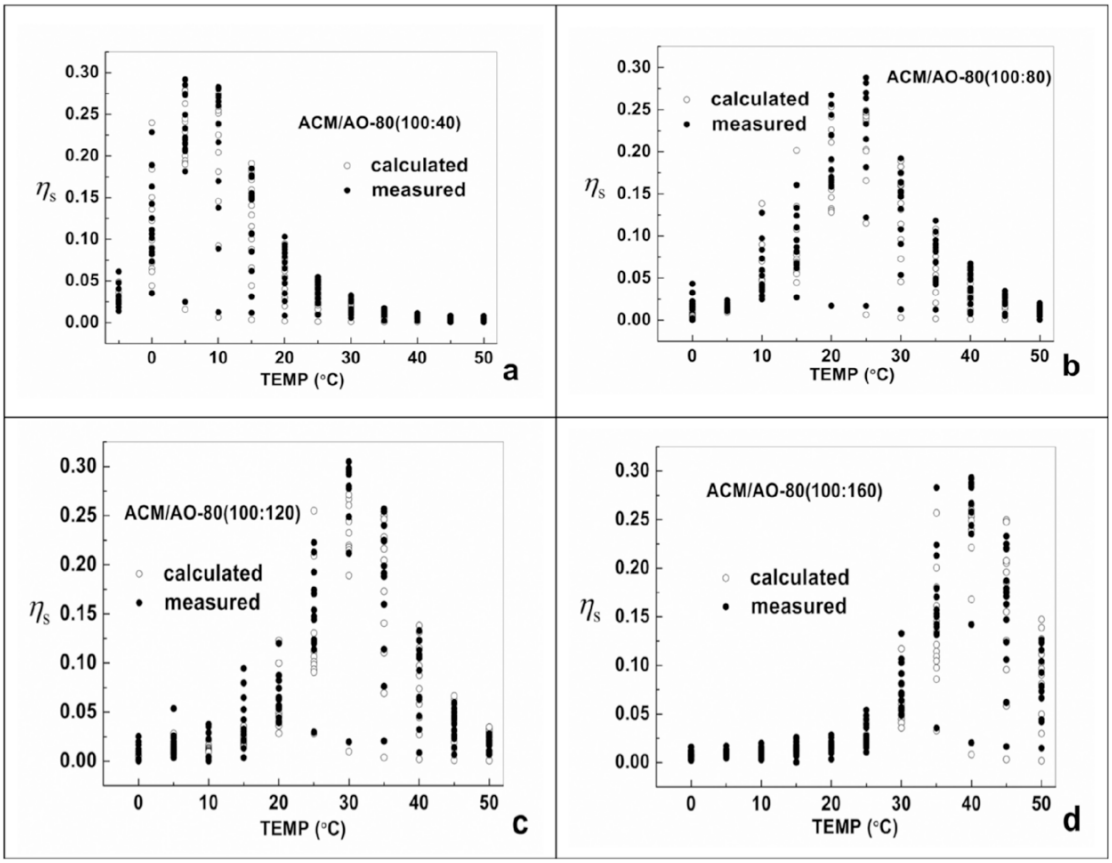


**Figure 13:** Temperature vs structural loss factor of different ACM/AO-80 hybrids laminated sandwich beams by DMA and theoretical model separately during a frequency range from 1 Hz to 600 Hz.

of AO-80 is similar to that of the tan $\delta$ peak temperature of the corresponding damping layer material, but the temperature appearing the $\eta_s$ peak is relatively lower. In this way, we can adjust the content of AO-80 to achieve a high damping property for sandwich beam at a pointed temperature during a frequency range from 1Hz to 600Hz, and the theoretical model proposed in this paper is an effective method to predict the possible position appearing the high damping property for the sandwich beam.

## 6. CONCLUSIONS

High damping materials were prepared by ACM/AO-80 hybrids. Hinder phenol AO-80 is very effective for improving the damping ability of ACM, and ACM/AO-80 hybrids were selected as the damping layer materials.

A new approach by DMA with a boundary condition that both ends of the beam are clamped with a concentrated sinusoidal load $P_0e^{i\omega t}$ applied at the midpoint of the constraining layer was used to measure the vibration damping behaviors of sandwich beams, and a theoretical model was established to characterize the damping behavior of the sandwich beam effectively. Though this method is different from the standard ASTM E 756-98, it can reflect the variation of structural loss factor with various factors. On the other hand, due to the popular application of DMA, it has the possibility to become a new way to measure the vibration damping behaviors of sandwich structures.

## REFERENCES

[1] Yamada N, Shoji S, Sasaki H, *et al*. Developments of high performance vibration absorber from poly(vinyl chloride)/chlorinated polyethylene/epoxidized natural rubber blend. J Appl Polym Sci 1999; 71: 855-63. http://dx.doi.org/10.1002/(SICI)1097-4628(19990207)71:6<855::AID-APP1>3.0.CO;2-V

[2] Wu J, Huang G, Wang X, Zhang J. Detecting different modes of molecular motion in polyisobutylene and chlorinated butyl rubber by using dielectric probes. Softer Matter 2011; 7: 9224-30. http://dx.doi.org/10.1039/c1sm05748k

[3] Huang GS, He XR, Wu JR, Pan QY, Zhen J, Hong Z. Effect of miscibility and forced compatibility on damping properties of CIIR/PAc blend. J Appl Polym Sci 2006; 102: 3127-33. http://dx.doi.org/10.1002/app.24252

[4] Liu M, Song G, Yi J, Xu Y. Damping analysis of polyurethane/polyacrylate interpenetrating polymer network composites filled with graphite particles. Polymer Composite 2013; 34: 288-92. http://dx.doi.org/10.1002/pc.22395

[5] Zhou X, Zhang G, Zhang W, Wang J. Studies on the damping properties of polyacrylate emulsion/hindered phenol hybrids. Polym J 2012; 44: 382-7. http://dx.doi.org/10.1038/pj.2012.6

[6] Zeng W, Li SC. Effect of components (acrynitril and acrylate acid) on damping properties of poly(styrene-acrynitril)/poly(ethylacetate-*n*-butylacrylate) latex interpenetrating polymer networks. J Appl Polym Sci 2002; 84: 821-6. http://dx.doi.org/10.1002/app.10350

[7] Saritha A, Joseph K. Effect of nano clay on the constrained polymer volume of chlorobutyl rubber nanocomposites. Polym Composites 2015; 36: 2135-9. http://dx.doi.org/10.1002/pc.23124

[8] Nugay N, Erman B. Property optimization in nitrile rubber composites via hybrid filler systems. J Appl Polym Sci 2001; 79: 366-74. http://dx.doi.org/10.1002/1097-4628(20010110)79:2<366::AID-APP220>3.0.CO;2-Y

[9] Song M, Zhao TX, Ishida Y, Wu S. Molecular dynamics simulations and microscopic analysis of the damping performance of hindered phenol AO-60/nitrile-butadiene rubber composites. RSC Adv 2014; 4: 6719-29. http://dx.doi.org/10.1039/c3ra46275g

[10] Wu CF, Yamagishi T, Nakamoto Y, Ishida S, Nitta K, Kubota S. Organic hybrid of chlorinated polyethylene and hindered phenol. I. Dynamic mechanical properties. J Polym Sci Pol Phys 2000; 38: 2285-95. http://dx.doi.org/10.1002/1099-0488(20000901)38:17<2285::AID-POLB90>3.0.CO;2-X

[11] Yin XT, Liu TCY, Lin Y, Guan AG, Wu GZ. Influence of hydrogen bonding interaction on the damping properties of poly(*n*-butyl methacrylate)/small molecule hybrids. J Appl Polym Sci 2015; 132: 41954-66. http://dx.doi.org/10.1002/app.41954

[12] Wu CF. Relaxation effects in an organic glassy material. J Non-Cryst Solids 2003; 315: 321-4. http://dx.doi.org/10.1016/S0022-3093(02)01910-5

[13] Nashif AD, Jones DIG, Henderson JP. Vibration Damping, John Wiley and Sons, Inc., New York, 1985.

[14] Liao FS, Hsu TJ. Prediction of vibration damping properties of polymer-laminated steel sheet using time-temperature superposition principle. J Appl Polym Sci 1992; 45: 893-900. http://dx.doi.org/10.1002/app.1992.070450516

[15] Öborn J, Bertilsson H, Rigdahl M. Styrene-Ethylene/Butylene-Styrene blends for improved constrained-layer damping. J Appl Polym Sci 2001; 80: 2865-76. http://dx.doi.org/10.1002/app.1404

[16] Li C, Xu SA, Xiao FY, Wu CF. Dynamic mechanical properties of chlorinated butyl rubber blends. Eur Polym J 2006; 42: 2507-14. http://dx.doi.org/10.1016/j.eurpolymj.2006.06.004

[17] Wu CF. Effects of hindered phenol compound on the dynamic mechanical properties of chlorinated polyethylene, acrylic rubber, and their blend. J Appl Polym Sci 2001; 80: 2468-73. http://dx.doi.org/10.1002/app.1354

[18] Edward M, Kerwin JR. Damping of flexural waves by a constrained viscoelastic layer. J Acoust Soc Am 1959; 31: 952-62. http://dx.doi.org/10.1121/1.1907821

[19] Plunkett R, Lee CT. Length optimization for constrained viscoelastic layer damping. J Acoust Soc Am 1970; 48: 150-61. http://dx.doi.org/10.1121/1.1912112

[20] Fan QC, Wang B, Yin YJ. Mechanics of Materials, Higher Education Press., Bei Jing, 2000.

Received on 23-11-2015 Accepted on 07-12-2015 Published on 18-04-2016

DOI: http://dx.doi.org/10.6000/1929-5995.2016.05.01.1